

Investigation and prediction of a roughness-induced, high-speed boundary-layer transition using machine learning

By O. Marxen[†], A. T. Margaritis[‡], P. J. Schmid[¶], T. J. Flint AND G. Iaccarino

A numerical investigation of disturbance amplification in a Mach-4.8 flat-plate boundary layer is performed, for which a two-dimensional discrete roughness has been placed on the surface. The effect of this roughness on disturbance behavior is quantified by comparing the disturbance amplification of a flat plate with and without the roughness. In addition to the perturbation frequency, the height, width and downstream location of the roughness are varied. Results have been obtained using a high-order finite-difference code that has previously been used for similar investigations. The simulation data are used to train a neural network that is shown to be able to quickly predict the effect of roughness on disturbance amplification. The trained neural network is found to achieve good accuracy at a fraction of the cost of the simulations, although these remain necessary to provide training data. In addition, an autoencoder approach is applied to the simulation data in order to gain insight into the mechanism underlying amplification in the presence of roughness. The results indicate that the two parameters, disturbance frequency and roughness location, influence amplification in such a way that both can likely be combined into a single parameter. Physical arguments discussed in the literature suggest that such a correlation should indeed exist, but the autoencoder is able to indicate such a correlation without any prior knowledge of the physics of the problem. Therefore, such an approach can be used to reduce the dimensionality of the parameter space and discover underlying correlations.

1. Introduction

Knowledge of the location of laminar-turbulent transition is relevant for a large number of technical applications. One particularly important application is the thermal-protection systems of hypersonic cruise and atmospheric (re)entry vehicles. For these vehicles, an accurate prediction of the transition location is crucial for the design of the thermal-protection system and the determination of its dimensions and materials. The development of credible engineering models for the prediction of laminar-turbulent transition is therefore a critical task.

Laminar-turbulent transition may occur in the absence of any form of intentional forcing as well as be triggered or influenced by roughness elements on the vehicle's surface (Berry & Horvath 2007; Schneider 2007; Greene *et al.* 2011; Chaudhry *et al.* 2015). Today's state-of-the-art methods for transition prediction yield a transition location for smooth surfaces. Two commonly used classes of methods are correlation-based methods (Reda 2002) and the e^N -method (Malik 1989). Recently, methods for transition prediction

[†] School of Mechanical Engineering Sciences, University of Surrey, United Kingdom

[‡] Department of Mathematics, Imperial College London, United Kingdom

[¶] King Abdullah University of Science and Technology, Saudi Arabia

based on machine learning (ML) have emerged (Zafar *et al.* 2021). Correlation-based methods rely on the averaging of empirical data, but Reshotko (2007) contends these methods, while widely used by vehicle designers, are not reliable and should be replaced by the e^N -method.

The e^N -method proposes that the most amplified disturbance and hence the supposedly most dangerous disturbance provides the most likely transition location. Typical N -factors at transition lie in the range of 5–10 (Malik 2003). While ML-based, the method proposed in Zafar *et al.* (2021) still relies on predicting disturbance growth on smooth surfaces only.

A stationary roughness of moderate height may significantly alter the boundary layer, but it does not directly introduce any time-dependent perturbation into the flow (Zhong & Wang 2012). Hence, in this situation the roughness acts as an amplifier of incoming disturbances rather than an oscillator. Convective amplification of these perturbations is typically increased in the wake of the roughness due to local boundary-layer deformation (Marxen *et al.* 2010a).

The effect of roughness on boundary-layer instability and hence on the N -factor can not be easily captured, since local linear stability theory is inaccurate in the vicinity of a 2-D roughness (Marxen *et al.* 2010a). Instead, a region of transient growth has been observed along and downstream of the roughness, which may significantly boost disturbance amplitudes. For 2-D roughness, Crouch (2008) proposed to account for growth modifiers by adding a ΔN to the N -factor. In this approach, the e^N analysis relies on a base flow without roughness in conjunction with 1-D (in the 2-D roughness case) stability theory.

The growth modifier ΔN for a given setup needs to be known with sufficiently high accuracy, as disturbance growth rates in the hypersonic regime are typically moderately large, suggesting that a small change in the ΔN can lead to a large shift in the transition location. At the same time, many applications, such as real-time estimation of transition during vehicle operation and optimization procedures, require the growth modifier to be not only accurate but also available quickly with short turnaround times.

The overarching goal of this project is therefore to develop a ML tool, trained with data from direct numerical simulation (DNS) to achieve high accuracy, that can subsequently be used for quick transition prediction.

2. Computational setup

2.1. Overview

Several parameters control the way a roughness influences the transition to turbulence, hence, a general classification of the types of roughness-induced transition is difficult. We will focus on the situation where the roughness is sufficiently tall that boundary-layer separation and weak shocks occur, but the roughness still interacts with the boundary layer only, and not directly with the freestream. This may happen for a ratio of roughness height to local boundary-layer thickness smaller than one. Due to the emergence of separation zones, linearization around a state composed of the boundary layer without roughness is typically not justified. At the same time, disturbances causing flow unsteadiness will typically remain a result of a linear convective growth mechanism. Hence, it is meaningful to linearize the flow field around a steady base state, justifying a focus on amplification rather than absolute amplitude and forcing disturbances with small amplitudes only.

Roughness height h_r	0.1, 0.2, ..., 1.0	10 values
Roughness length l_r	0.2, 0.4, 0.6, 0.8, 1.2, 1.6, 2.4, 3.2	8 values
Roughness location x_r	10.0, 12.5, 15.0, 17.5, 20.0	5 values
Frequency parameter F	24, 36, 48, 60, 70	5 values

TABLE 1. Geometric parameters of the roughness and disturbance frequencies.

2.2. Numerical method for simulations

In order to obtain results, a high-order finite-difference method, together with explicit fourth-order Runge-Kutta time integration, is used. The compressible Navier-Stokes equations are solved for a calorically perfect gas on a curvilinear grid. The numerical method is described in detail in Nagarajan *et al.* (2003) and Marxen *et al.* (2010a), and the code has previously been used to investigate hypersonic boundary-layer transition (Marxen *et al.* 2010a,b, 2014b; Ryu *et al.* 2015). While the solver is capable of including finite-rate chemistry models and real-gas thermodynamic and transport properties (Marxen *et al.* 2011, 2013, 2014a; Margaritis *et al.* 2022), this report is only concerned with a calorically perfect gas.

The present method is similar to the one applied for investigations of uncertainties of roughness height in Marxen *et al.* (2010b). Due to a large number of test cases, runs were performed on a compute cluster using SLURM_ARRAY, which significantly simplified running the simulations with varying parameters.

2.3. Test cases

The test case under consideration is similar to that studied in Marxen *et al.* (2010a). A 2-D, rounded rectangular roughness is placed on the surface of a flat plate, which is subject to a supersonic free freestream with a Mach number $Ma = 4.8$. Details of the setup, including grid and domain sizes, can be found in Marxen *et al.* (2010a). Unlike in that reference, geometric parameters of the roughness are varied more widely and systematically. Table 1 provides an overview of the parameter values used in simulations here.

Forcing amplitudes for the perturbation were chosen such that there was no interaction between the different frequencies, despite some frequencies being higher harmonics of lower forced frequencies. As a result, a single numerical simulation with a fixed roughness geometry contributed results for all five frequencies. Therefore, a total of $10 \times 8 \times 5 = 400$ simulations were required to obtain all data. Each simulation was run on 80 CPUs and took about 3 h. However, not all simulations could be completed, such as those for the tallest roughness ($h_r = 1.0$); these will likely require the use of a shock-capturing scheme. Simulations were advanced in time until a statistically steady state was reached, followed by a Fourier transform in time (for a description of data processing see Marxen *et al.* 2010a). Convergence was judged by inspecting the amplitude of a subharmonic $F = 12$, which should be sufficiently below the amplitude of the forced perturbations. Figure 1 gives an overview of all the cases, including parameter values. The bottom panel in the figure illustrates the five different frequencies F used, whereas the panel above corresponds to the eight different lengths of the roughness l_r . The center panel specifies the roughness heights h_r , and for every frequency F and roughness length l_r , ten different heights h_r were computed. Finally, the panel with axis label x_r shows the range of roughness locations x_r , and for each F , l_r and h_r , five different values for x_r were used.

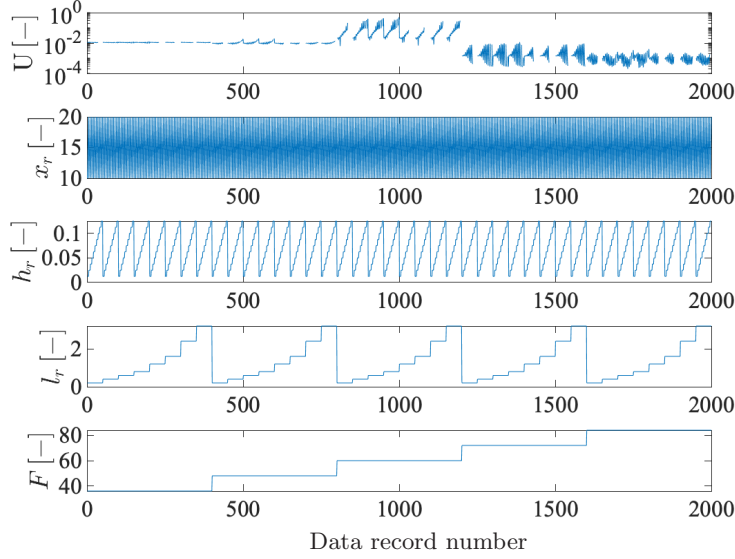


FIGURE 1. Illustration of simulation parameter variations (bottom four panels) and simulation results for the maximum amplitude of the streamwise perturbation at downstream Reynolds number $R_x = 2000$ (top panel).

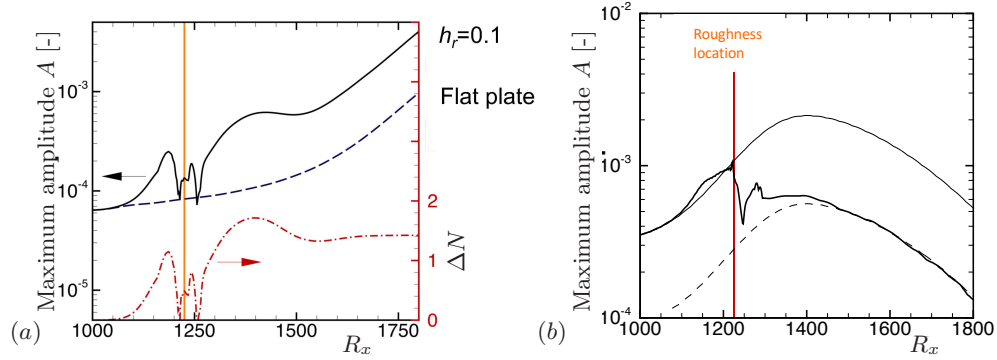


FIGURE 2. Maximum amplitude for flat-plate (thin/dashed) and roughness cases ($h_r = 0.1$, $l_r = 0.4$ and $x_r = 15$) for two different frequencies (a) $F = 48$, together with the resulting ΔN , and (b) $F = 72$.

2.4. Postprocessing

The presence of a roughness alters the amplitude of the perturbation wave (Figure 2). Depending on the parameters of the setup, an increased [Figure 2(a)] or decreased [Figure 2(b)] amplification is observed. The difference in amplification between flat-plate flow and flow in the presence of a roughness is quantified using the following equation (Marxen *et al.* 2010b)

$$\Delta N = \ln \left. \frac{A_R}{A_{FP}} \right|_{x=40}.$$

Far downstream of the roughness, the amplification rate for cases with roughness approaches that of a flat plate. As a result, ΔN becomes constant [Figure 2(a); $R_x = \sqrt{Re \times x} > 1600$] so that the choice of streamwise location (here $x = 40$) is not important. Similarly, the dashed (auxiliary) line in Figure 2(b) corresponds to the flat-plate case but has been shifted by a factor, and it is observed to match the results with roughness (thick, solid line).

2.5. Methods for machine learning

A neural-network-based prediction tool has been implemented in MATLAB using built-in functions with three layers and 25, 20 and 15 neurons per layer, respectively. A nonlinear tanh activation function has been chosen. For training, the postprocessed data set described in the previous section was used, i.e., the five input parameters disturbance frequency, roughness height, length and location, together with ΔN as output variable, using a nonlinear autoencoder implemented in Python. The autoencoder was trained with a reduced data set, where only data for varying disturbance frequency and roughness length have been used for a fixed roughness height ($h = 0.1$) and location ($x_r = 15$). This approach was taken to explore whether these two parameters could be reduced to a single one.

3. Results

In this section, DNS results will be discussed. First, in Section 3.1, the effect of parameter variations will be discussed in order to gain additional insight into the effect of a 2-D roughness on boundary-layer instability. The next section (Section 3.2) discusses how well a neural network trained with these DNS data is able to predict the amplification altered by the presence of roughness, given its geometrical parameters and the frequency. Finally, Section 3.3 investigates how the application of an autoencoder can help gain additional insight into the flow physics for the present case.

3.1. Parametric effects

In order to illustrate parametric effects, Figure 3 depicts disturbance amplification if a single parameter is varied while all others are kept fixed. Figure 3(a) illustrates the dependency of amplification on frequency. Data presented in the figure result from a single simulation, in which five different frequencies have been forced in the disturbance strip upstream of the roughness. Whereas moderate or even strong amplification in the downstream direction is observed for some frequencies, perturbations for other frequencies exhibit a strong decay downstream of the roughness. The figure shows that for strong decay, a fully statistically steady state is not reached (nonsmooth green line). Nonetheless, since strongly damped perturbations are not expected to play a central role for laminar-turbulent transition, such a level of convergence was deemed acceptable. Figure 3(b) combines the results of several different simulations in which the roughness location and length were kept fixed, but the roughness height was varied. Only results for a single frequency are shown. A strong variation of final amplitude is observed, suggesting that the flow is sensitive to both height and location of the roughness. However, this sensitivity decreases for the largest heights considered, confirming that for the present choice of roughness heights increased amplification is not proportional to roughness height. Figure 3(c) also combines the results of simulations with three of the four parameters fixed, but this time the roughness length was varied. While amplification differs in the vicinity of the roughness, the effect on disturbance amplitude attained far downstream is

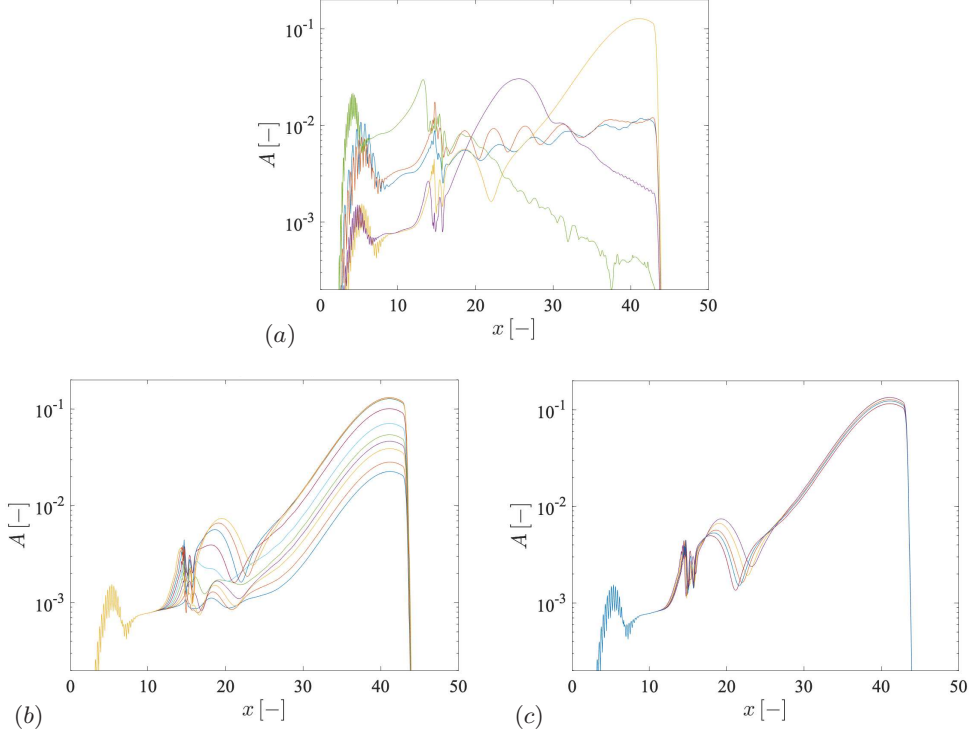


FIGURE 3. Maximum amplitude for (a) frequency variation (for $x_r=15$, $l_r=0.4$ and $h_r=0.1$), (b) roughness height variation (for $x_r=15$, $l_r=0.4$ and $F=48$) and (c) roughness length variation (for $x_r=15$, $h_r=0.4$ and $F=48$).

small. However, for other parameter combinations the effect of roughness length is more pronounced (not shown here).

3.2. Prediction

This section serves to assess the ability of the neural network trained with DNS data to accurately predict the effect of roughness on disturbance amplification. Figure 4 compares DNS results with those obtained using the trained neural network. The figure shows that the neural network can accurately capture the effect of the roughness height variation. The figure also highlights that, unlike what was seen in Figure 3(b), there is not always a monotonic dependence of disturbance amplification on roughness height. Instead, there can even be a qualitatively different effect of roughness height on perturbation amplitude, with small roughness heights leading to an increase of amplification and larger heights damping the perturbation when compared to a flat-plate setup. This observation underlines that a prediction tool such as the present one may be useful to support the design of roughness-based flow-control strategies. In contrast to the time it took to perform each individual simulation on a compute cluster, the trained neural-network-based model could be run on a standard laptop and would reach its prediction within seconds, further highlighting its potential usefulness. However, its performance for extrapolation has not yet been checked.

Figure 5 illustrates a further validation of the performance of our neural network by comparing the response predicted by the network with exact results (which correspond

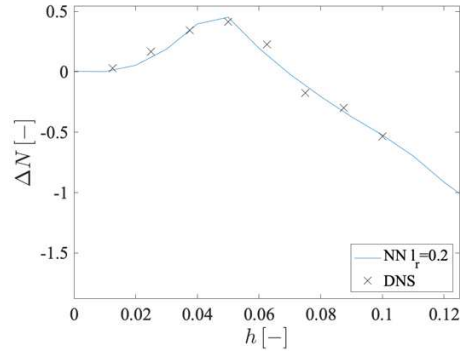


FIGURE 4. Comparison of DNS results and neural-network (NN) prediction for fixed frequency, fixed roughness length and location but varying height.

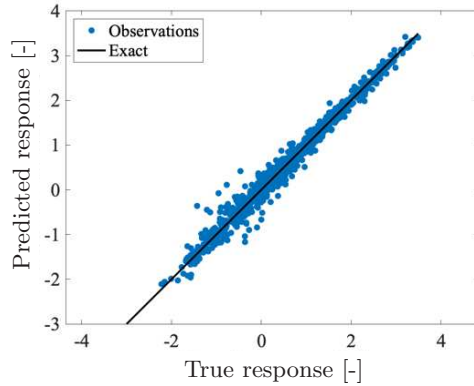


FIGURE 5. Validation of the neural network approach by plotting the ΔN response predicted by the neural network (labeled Observations) versus the true response (DNS data), with the black line indicating the exact case.

to DNS data) for all chosen parameters. Overall excellent performance of the neural network approach can be seen, with only small deviations from the exact results even for largest values of ΔN . Performance appears to be at its worst around the origin, i.e., when the differences between roughness and flat-plate cases are smallest. However, these cases are not deemed particularly relevant for applications such as worst-case transition prediction or optimal flow control.

3.3. Toward an understanding of roughness effects

It has been argued that “judiciously placed roughness elements downstream of the synchronization point can damp the most amplified disturbances.” (Fong *et al.* 2015, p. 3142) The synchronization point corresponds to the streamwise location at which the phase speed of the fast and slow boundary-layer perturbation modes, originating from slow and fast acoustic waves at the plate’s leading edge, match. This location depends on the disturbance frequency, and therefore we expect to find that both disturbance frequency and roughness location may have similar effects on disturbance-amplitude alteration caused by the roughness. However, the results of Figure 4 showed that the effect of roughness on disturbance damping is more complex than can be explained by roughness location, and

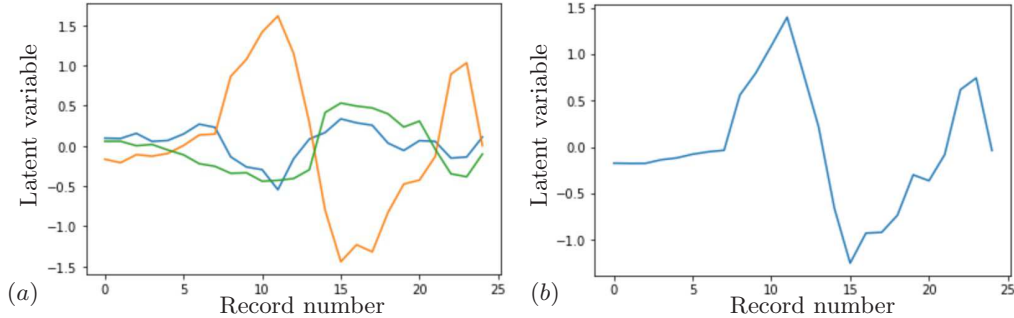


FIGURE 6. Autoencoder results for a latent space of (a) three variables and (b) one variable.

therefore it is important to gain further insight into the physical processes underlying the interaction of roughness and boundary-layer perturbation. Still, the aforementioned observation motivates the application of an autoencoder to the DNS data in order to learn more about the corresponding parameters, disturbance frequency and roughness location.

The DNS data was restricted to a case in which the frequency and the roughness location were varied for a fixed roughness height and width. As both five frequencies and wave locations had been considered in our DNS data set, this resulted in a data set of 25 entries. The data record containing 25 entries was then used to train an autoencoder with one and three latent variables.

Figure 6 depicts values of latent variables as a function of record number. Figure 6(a) indicates that a single latent variable can explain most of the variation of ΔN . The remaining two variables are roughly a factor of three lower in maximum value while having a similar dependence on record number, albeit with a different sign. This latter observation indicates that these two latent variables may be linearly dependent on the first one, and hence that a single (latent) variable may be sufficient to capture the variation of the data. Indeed, when the latent space is reduced to a single variable [Figure 6(b)], the resulting shape is very similar to that observed for the most dominant latent variable in the case with a latent space of three [compare Figure 6(a)]. This observation further supports the hypothesis that a single parameter, combining disturbance frequency and roughness location, may determine the effect of roughness on amplification.

4. Conclusions

An extensive database for the amplification of boundary-layer perturbations in a supersonic flow with 2-D surface roughness has been generated, considering four different parameters related to disturbance frequency and roughness geometry, including roughness height, width and location. Trained with this data, a neural-network-based prediction tool was able to accurately predict the alteration of amplitude caused by the roughness. Not only does this prediction tool provide accurate results, but its results can also be obtained with minimal computational resources required. While obtaining training data is associated with significant computational costs, the trained neural network is able to predict the effect of roughness with high accuracy at a fraction of the cost of performing even a single numerical simulation. The prediction tool is therefore able to support applications that require real-time decision-making or quick turnaround times for geometric optimization.

In the future, the present work should be extended to include 3-D simulations results. A central assumption underlying this report is that laminar-turbulent transition is driven by the amplification of 2-D boundary-layer waves. The proxy parameter used here, namely an increased amplification caused by the roughness, relies on the rapid occurrence of secondary instabilities. While the experimental work by Fong *et al.* (2015) shows that this assumption may indeed hold and that the proxy parameter used here is indeed relevant, it may be useful to consider the full laminar-turbulent transition process by performing 3-D simulations.

Although the DNS database was generated mainly with the purpose of training the prediction tool, additional insight into the effect of parameter variations could be gained. In particular, it was found that roughness height may play a role in determining whether the roughness causes disturbance amplification or damping. The application of an autoencoder to the DNS data highlighted its potential to provide further insight into parametric effects. While these results are encouraging, additional work needs to be performed, in particular with respect to regularization. Also, while the autoencoder indicated that the combination of roughness location and disturbance frequency could be collapsed into a single parameter, the structure of this parameter remains unknown.

Acknowledgments

The authors acknowledge use of computational resources from the Yellowstone cluster awarded by the National Science Foundation to CTR.

REFERENCES

- BERRY, S. A. & HORVATH, T. J. 2007 Discrete roughness transition for hypersonic flight vehicles. *AIAA Paper* **2007-0307**.
- CHAUDHRY, R. S., SUBBAREDDY, P. K., NOMPELIS, I. & CANDLER, G. V. 2015 Direct numerical simulation of roughness-induced transition in the VKI Mach 6 tunnel. *AIAA Paper* **2015-0274**.
- CROUCH, J. D. 2008 Modeling transition physics for laminar flow control. *AIAA Paper* **2008-3832**.
- FONG, K. D., WANG, X., HUANG, Y., ZHONG, X., MCKIERNAN, G. R., FISHER, R. A. & SCHNEIDER, S. P. 2015 Second mode suppression in hypersonic boundary layer by roughness: Design and experiments. *AIAA J.* **53**, 3138–3144.
- GREENE, P. T., ELDREDGE, J. D., ZHONG, X. & KIM, J. 2011 Numerical study of hypersonic flow over an isolated roughness with a high-order cut-cell method. *AIAA Paper* **2011-3249**.
- MALIK, M. R. 1989 Prediction and control of transition in supersonic and hypersonic boundary layers. *AIAA J.* **27**, 1487–1493.
- MALIK, M. R. 2003 Hypersonic flight transition data analysis using parabolized stability equations with chemistry effects. *J. Spacecr. Rocket.* **40**, 332–344.
- MARGARITIS, A. T., SCHERDING, C., MARXEN, O., SCHMID, P. J. & SAYADI, T. 2022 Development of a high-fidelity computational tool for chemically reacting hypersonic flow simulations. arXiv:2210.05547.
- MARXEN, O., IACCARINO, G. & MAGIN, T. E. 2014a Direct numerical simulations of hypersonic boundary-layer transition with finite-rate chemistry. *J. Fluid Mech.* **755**, 35–49.
- MARXEN, O., IACCARINO, G. & SHAQFEH, E. S. G. 2010a Disturbance evolution in

- a Mach 4.8 boundary layer with two-dimensional roughness-induced separation and shock. *J. Fluid Mech.* **648**, 435.
- MARXEN, O., IACCARINO, G. & SHAQFEH, E. S. G. 2010*b* Linear and non-linear disturbance evolution in a compressible boundary-layer with localized roughness. In *Seventh IUTAM Symposium on Laminar-Turbulent Transition* (ed. G. M. L. Gladwell, R. Moreau, P. Schlatter & D. S. Henningson), *IUTAM Bookseries*, vol. 18, pp. 271–276. Springer Netherlands.
- MARXEN, O., IACCARINO, G. & SHAQFEH, E. S. G. 2014*b* Nonlinear instability of a supersonic boundary layer with two-dimensional roughness. *J. Fluid Mech.* **752**, 497–520.
- MARXEN, O., MAGIN, T. E., IACCARINO, G. & SHAQFEH, E. S. G. 2011 A high-order numerical method to study hypersonic boundary-layer instability including high-temperature gas effects. *Phys. Fluids* **23**, 084108.
- MARXEN, O., MAGIN, T. E., SHAQFEH, E. S. G. & IACCARINO, G. 2013 A method for the direct numerical simulation of hypersonic boundary-layer instability with finite-rate chemistry. *J. Comput. Phys.* **255**, 572–589.
- NAGARAJAN, S., LELE, S. K. & FERZIGER, J. H. 2003 A robust high-order method for large eddy simulation. *J. Comput. Phys.* **191**, 392–419.
- REDA, D. C. 2002 Review and synthesis of roughness-dominated transition correlations for reentry applications. *J. Spacecr. Rocket.* **39**, 161–167.
- RESHOTKO, E. 2007 Is Re_θ/M_e a meaningful transition criterion? *AIAA J.* **45**, 1441–1443.
- RYU, S., MARXEN, O. & IACCARINO, G. 2015 A comparison of laminar-turbulent boundary-layer transitions induced by deterministic and random oblique waves at Mach 3. *Int. J. Heat Fluid Flow* **56**, 218–232.
- SCHNEIDER, S. P. 2007 Effects of roughness on hypersonic boundary-layer transition. *AIAA Paper* **2007-0305**.
- ZAFAR, M. I., CHOUDHARI, M. M., PAREDES, P. & XIAO, H. 2021 Recurrent neural network for end-to-end modeling of laminar-turbulent transition. *Data-Centric Eng.* **2**, e17.
- ZHONG, X. & WANG, X. 2012 Direct numerical simulation on the receptivity, instability, and transition of hypersonic boundary layers. *Annu. Rev. Fluid Mech.* **44**, 527–561.